

Child Neck FE Model Development and validation

Meyer F., Roth S., Willinger R.

(Strasbourg University, ULP-CNRS 7507, 2 rue Boussingault, 67000 Strasbourg, France, E-mail : meyer@imfs.u-strasbg.fr)

Abstract: Despite of recent progresses in occupant safety, the protection of children is not still optimal. To offer a better understanding of child injury mechanisms, the present study proposes a human-like finite element model of a three years old child's neck. The subject was scanned with a medical scanner. The images were first semi-automatically segmented in order to extract the soft tissues and the bones. In a second step, the different bones were separated slice by slice on the geometry previously reconstructed. The anatomic structures are identified and each vertebra is reconstructed independently with special attention for the articular process. Finally, an original meshing on the previous geometry was generated to obtain a finite element model of the child's neck. For validation purpose, the FEM response was superimposed with time corridors available in the literature for different impact cases, which have been scaled down using adapted scale factors from Irwin and Mertz (1997).

Keywords: Finite element neck model, Scaling Method, Child biomechanics.

1 Introduction

Each year, more than 700 children are killed on European roads and 80.000 are injured. The EC project CHILD (Child Injury Led Design) aims to improve the protection offered to children in cars by increasing the understanding of the injuries sustained and providing innovative tools and methods for improvement of Child Restraint Systems (CRS) in cars. One of the tools developed is a realistic three year old child neck finite element model. No paediatric neck finite element models exist yet, because of the lack of data allowing validations. However, Irwin developed the "scaling method" to obtain dynamic child response from adult response. They used adapted scale coefficients depending on the age of the child and scaled recorded accelerations and displacements. Tests carried out by the N.B.D.L. (National BioDynamics Laboratory) for frontal, lateral, oblique (Ewing et al. 1968 [1] and Ewing et al. 1977 [2]) as well as rear impacts (Prasad et al. 1997 [3]) for adult neck were scaled down and used in the present child neck validation procedure.

Concerning the state of the art in this domain, only three human-like child cervical spine models were found in the literature. The first was developed by Kumaresan et al. (1997) [4] who developed three types of finite element models for three different ages (1, 3 and 6 years). These models were limited to the cervical C4–C6 segment and resulted directly from the adult geometry. It must be noticed that this adult model was developed in order to perform static simulations. Several types of model construction were adopted using a pure geometrical scaling, the introduction of anatomical specificities without any scaling, and models using scaling of geometry and mechanical properties simultaneously. For the first approach a pure geometrical scaling of the adult finite element model was proposed. No geometrical modification and no anatomical specificity according to the age were introduced in the model. Constitutive laws for the ligaments and the discs were not scaled, but maintained similar to those of adult. For computing and meshing reasons (divergence of the model), it was impossible to conduce a "scaling down" of the model, i.e. a scaling factor lower than 1. In order to solve this problem, the authors decided to realize a "scaling up" at 120, 140, 160 and 180%. The results were then extrapolated by supposing that the answer is linear according to the scaling coefficient and thus of the age. For the second approach, it was decided not to apply any scaling factor to the geometry of the adult. The meshing was thus identical to the adult's one but ligaments properties (stiffness) were modified in order to study their influences. In the last approach, scaling was used both on geometry and material properties to integrate anatomical specificities with regard to the age. The comparison of the three types of models was done under static conditions by applying either a compressive force (100 and 400 N), or a moment (0,25 and 1 Nm) at the top of C4, with C6 fixed, and by measuring the main range of motion compared to that of the adult. It appeared that there was a rigidification of the spinal segment studied with regard to the age, the 1-year-old child being much more flexible than the 6-year-old child. Moreover, it has been noticed that the independent parameters which lead to the highest increase in mobility were anatomical specificities and constitutive laws, rather than simple dimensional scaling, the combination of the two approaches yielding the highest mobility increase. Nevertheless, even though the observed trends seemed to be in conformity with the experimental results on animals, no experimentation on child is available to validate these results quantitatively, a limitation which the authors concede readily. Finally, even if these models were not validated, it should be noticed that the inclusion of geometrical specificities of the child's neck can be helpful in the understanding of the injury mechanisms. The other 3-year-old child finite element model found in the literature was developed by Mizuno et al. (2004) [5] by scaling down a global human finite element model to investigate the potential injury risks from restraints. The last finite element model of child neck has been developed by Dupuis et al. (2006) and was scaled down from adult model [6]. Its validation was performed against crash test dummy component sled tests. The accelerometric responses of the head model were similar to those recorded experimentally with a Q3 dummy neck in backward, frontal and lateral impact direction.

2 Model development

2.1 Model geometry

A three year old male child head and neck was scanned in order to base this study on a realistic human geometry and to integrate the detailed vertebrae anatomy. The 3-Year-old child was scanned for clinical reasons and had no cervical abnormalities. The 1.1 mm slices (figure 1) were first segmented semi-automatically in order to extract skin and bones and to reconstruct the geometry. This file was then imported under Hypermesh V7.0 a meshing software. The surfaces were reconstructed, as illustrated in figure 2 so that the cervical vertebrae could be completely meshed. Indeed, the explicit finite element calculation codes used in the crash field and in this study, Radioss 4.4 (Altair©), require regular meshing that fulfils geometrical criteria influencing the computation time pitch. Table 1 summarizes the values of these criteria used throughout the meshing process.

The cervical vertebrae were modelled using shell elements, the intervertebral discs with brick elements and the ligaments with

spring elements. The modelling option for vertebra is justified as shell elements offer the possibility to strictly respect the anatomical surface and to declare this part as a rigid body in order to respect the geometry of the articular surfaces and to correctly reproduce the inertias, even if the rigid body cannot reproduced fracture. For the facet interaction, the contact was reproduced with a sliding interface.

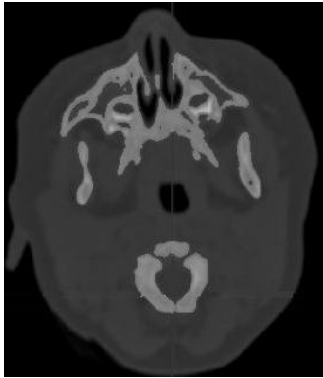


Figure 1: Scanner slices treatment step for the 3D reconstruction of the cervical spine.



Figure 2: Surface (igs) of the cervical vertebrae.

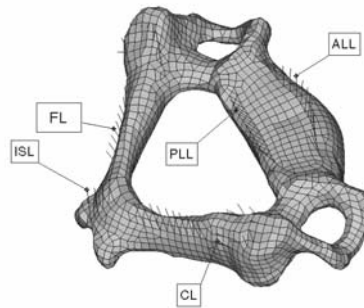


Figure 3: Ligamentary system of the lower spine (with the anterior longitudinal ligament (ALL), the posterior longitudinal ligament (PLL), the flavum ligament (FL), the interspinous ligament (ISL) and finally the capsular ligaments (CL).

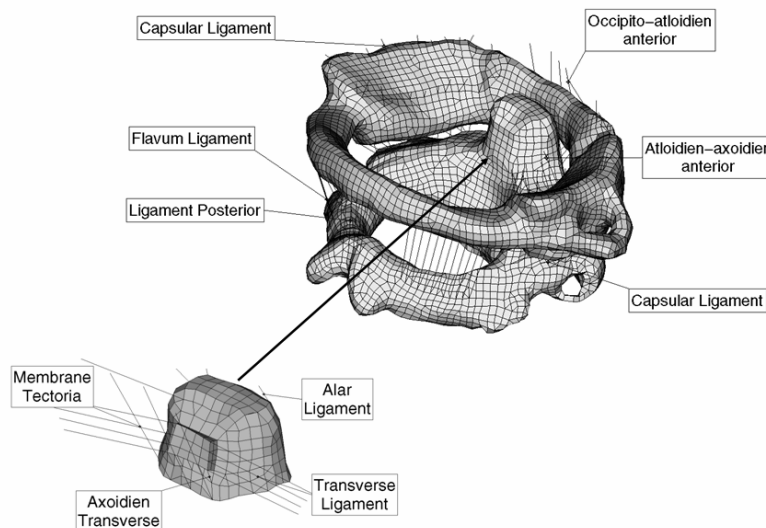


Figure 4: Ligamentary system of upper cervical spine (Atlas-Axis).

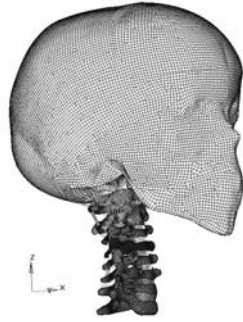


Figure 5: Finite element model of the 3-year-old child head-neck system.



Figure 6: Surface meshing of the cervical column (C1-T1) with its ligamentary system.

As far as the lower cervical spine is concerned, five types of ligaments were distinguished as shown in figure 3 i.e. the anterior longitudinal ligament (ALL), the posterior longitudinal ligament (PLL), the flavum ligament (FL), the interspinal ligament (ISL) and finally the capsular ligaments (CL).

For the upper cervical spine, the posterior common ligament (C2-C0; C2-C1; C1-C0), the atlodien-axoidien anterior ligament, the transverse ligament, the yellow ligament (C2-C1), the transverse axoid ligament, the anterior occipito-atloid ligament, the alar ligament, the posterior occipito-atloidien ligament, the capsular ligament C2-C1, the capsular ligament Head-C1, membrane tectoria, the median occipito-odontoid ligament as well as the lateral occipito-atloidien ligament were modelled as illustrated in figure 4.

The option to represent the intervertebral discs with bricks elements (3 layers) is justified by the need to reproduce the 3D shearing behaviour of this structure. Finally, a simplified head model is connected to the cervical column in order to integrate its mass and inertia effect. Its inertial properties are given in table 4.

As a whole, the finite element model of the head-neck system thus defined consists of 48 296 elements divided into 44 758 shell elements, 712 non linear spring elements and 2 826 volume elements. A more global representation of the model is given in figures 5 and 6.

2.2 Mechanical properties

Very limited mechanical properties on paediatric organs exist in the literature. For this reason, a scaling method has been developed to obtain mechanical properties of child organs from adult ones. Irwin and Mertz (1997) [7] worked on this method and found different coefficients for neck and head. Those scaling factors are applied to the adult head-neck system in order to obtain child head neck mechanical properties.

The constitutive laws of each ligament in both the lower and upper cervical spines, are defined by referencing two complementary studies, i.e. Chazal et al. (1985) [8] and Yoganandan et al. (2001) [9]. Chazal et al. (1985) study highlights the non-linear viscoelastic behavior of ligaments. Yoganandan et al. (2001) gives information on their failure properties. The overall behaviour of the ligaments can then be characterized by three points in the force versus deformation curve i.e. α_1 , α_2 , α_3 , determining respectively the limit of the neutral zone, the linear part, and finally the plastic behavior. It is supposed in this study that only the failure properties are lower for the child but that the viscoelastic behavior is remained.

The coefficients used for the present model are reported in table 2 and a representation of the typical behavior of the five ligaments of the lower cervical spine is illustrated in figure 7.

In order to take into account the initial lengths of the ligaments in the model as well as those measured anatomically by Yoganandan et al. on the lower cervical spine (2001) the following laws were calculated :

$$\begin{cases} d_i = \alpha_i * L * \left(\frac{L_m}{L} \right) \\ F_i = \frac{F_3 * \alpha_i}{N_{spring}} * \left(\frac{L_m}{L} \right) \end{cases} \quad i = 1, 2, 3$$

Where d_i is the spring elongation, F_i the force, N_{spring} the number of springs, L the experimental ligament length and L_m the mean length spring in the model. For the upper ligaments the initial experimental lengths are not given by Yoganandan et al. (2001), so the ratio between the initial length of the model and experimental are equal to 1. According to Irwin et al. (1997) and Yoganandan et al. (2000) [10] scaling factors, all ligaments behaviour laws were scaled in terms of force. Their mechanical properties are detailed in table 2. Most of neck FE models use an elastic law for the intervertebral discs and a wide range of Young's Modulus values has been observed in the literature, varying from 3.4 MPa in Yoganandan's model to 200 MPa in Dauvilliers' one [13]. Based on an adult young modulus and taking the scale factor of 0.705 given by Yoganandan (2000) for the 3-Year old child intervertebral discs as reference, we adopted a disc modulus of the order 100 MPa with a Poisson's ratio of 0.3.

The child mechanical characteristics in terms of mass and inertias for the head and neck are taken from the work reported by Deng et al. (1987) [11], scaled down using scale factors from Irwin (1997) and reported in table 3. Based on characteristic length ratio $\lambda_i (i = x, y, z)$, mass ratio λ_m , and mass density ratiom λ_p , linked by the following equation, new inertial properties of child vertebrae are found and listed in table 4.

$$\lambda_x = \lambda_y = \left[\frac{\lambda_p * \lambda_m}{\lambda_z} \right]^{\frac{1}{2}}$$

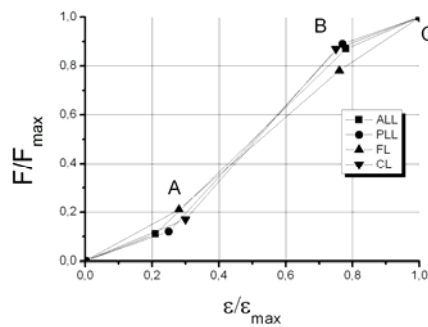


Figure 7: Behaviour laws of the anterior longitudinal ligaments, ligament (ALL C2-C5), posterior longitudinal ligament (PLL C2-C5), flaval ligament (FL C2-C5), interspinous ligament (ISL C2-C5), capsular ligament (CL C2-C5) issu from Chazal et al. (1985)

2.3 Model validation

Finite element models of adult necks are typically validated against experimental data carried out by the N.B.D.L., with frontal, oblique, lateral impacts on adult (Ewing et al. 1968). The advantage of the N.B.D.L. tests is that they are well instrumented tests carried out on volunteers and quite violent (15g for 100 ms). Unfortunately, it is not possible for ethical reasons to perform similar tests on children. No data exist in the literature for dynamic validation of a paediatric neck models.

A new original validation method can then be applied for child neck, based on existing experimental tests on adults, using the "scaling method" developed by Irwin et al (1997).

In the present study, inputs for the three-year-old-child model reported on figure 8 correspond to inputs used in the N.B.D.L. tests on adult. The model is submitted to different imposed velocity depending on impact load (frontal, lateral, oblique rear impact of N.B.D.L tests) (figure 8), applied at T1.

Outputs, i.e., head accelerations and displacements corridors for adult, are scaled down in accordance with Irwin's method. In this earlier study, several coefficients are proposed as a function of age. For the 3 YO (3 year old child), the geometrical scaling coefficients are detailed in table 3, and finally the ratio of accelerations is inversely proportional to the characteristic length ratio:

$$R_a = 1/\lambda_x$$

Finally, new validation curves for child neck, based on adult experimentations are obtained and used to validate the model under frontal, lateral, oblique and rear impact.

The following curves (figure 9 to 12) show the superimposition of experimental response (corridors) obtained with the scaling method, and numerical curves obtained with the new finite element model of the child neck under respectively frontal, rear, lateral, oblique impact. For each of these four figures, model validation is expressed in term of head acceleration and head/T1 relative displacement. The kinematics of the whole head/neck system is reported as well for each impact configuration."

In order to provide a quantitative model validation, statistical analysis have been performed on the response of the FEM, for each impact configurations.

For the frontal impact, a good correlation is observed in term of displacement (73% for x-displacement, and 99% for z-displacement). In terms of acceleration, 52% and 45 % of the response respectively in terms of x-linear acceleration and z-linear acceleration are included in the experimental corridor.

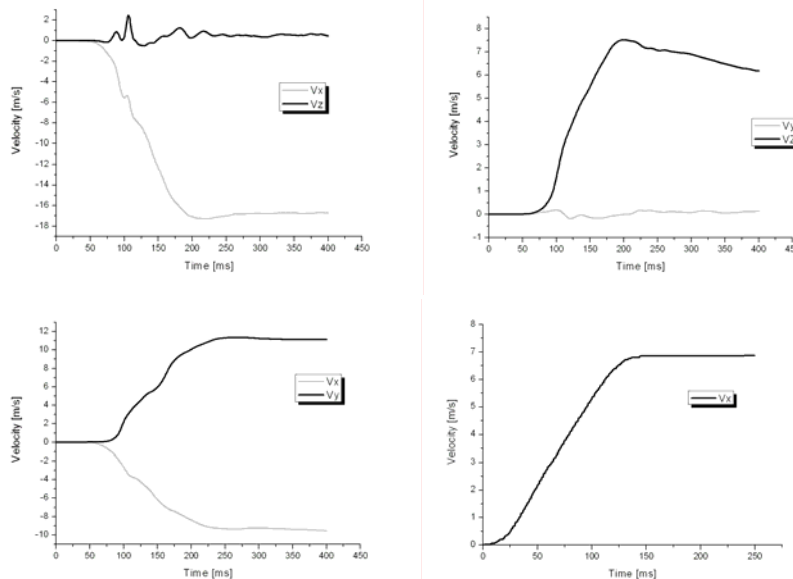
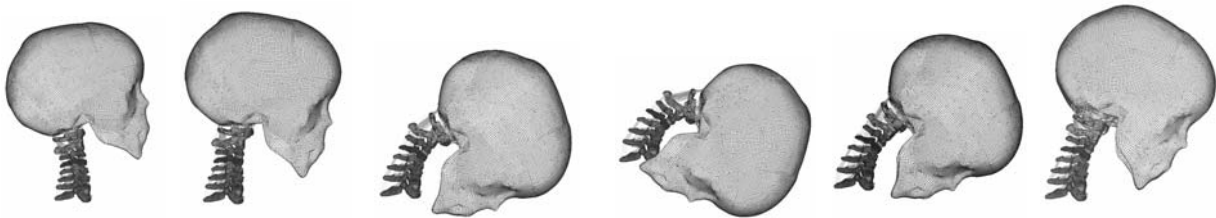
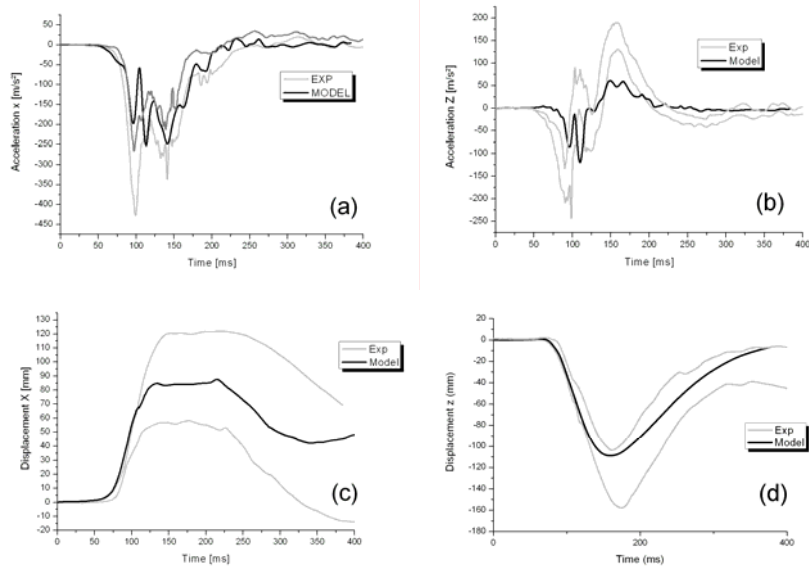
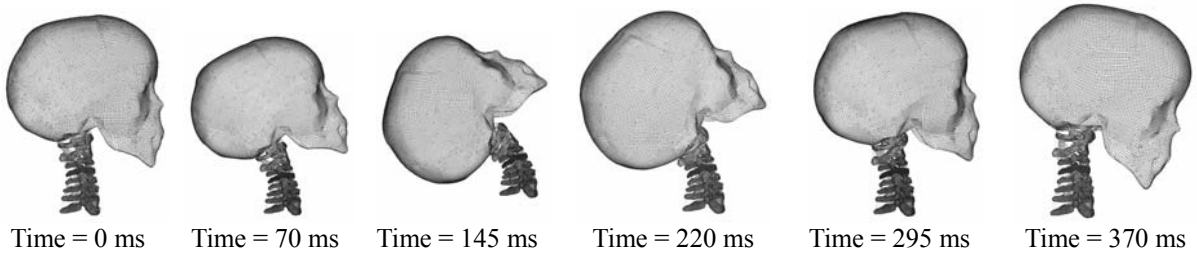
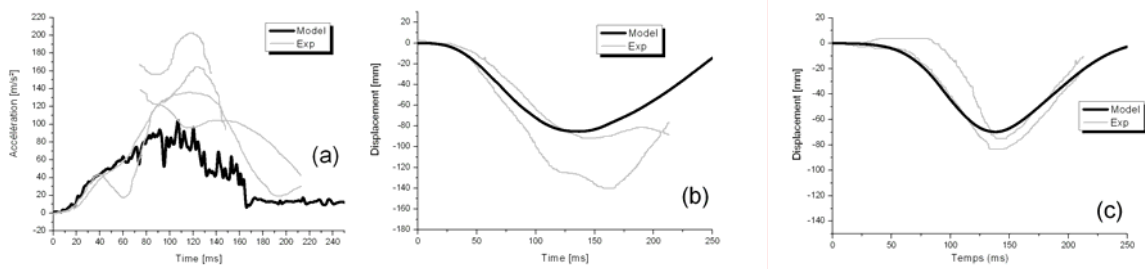


Figure 8: Imposed speed at T1 in case of frontal impact (a), lateral impact (b), oblique impact (c) and rear impact (d)



Time = 0 ms Time = 95 ms Time = 130 ms Time = 160 ms Time = 295 ms Time = 395 ms

Figure 9: Results under frontal impact: X-axis (a), Z-axis (b) linear head acceleration, X-axis (c), Z-axis (d) head displacement and kinematic response of the whole head/neck system (e).



Time = 0 ms Time = 70 ms Time = 145 ms Time = 220 ms Time = 295 ms Time = 370 ms

Figure 10: Results under rear impact: global head acceleration (a), X-axis (b), Z-axis (c) head displacement and kinematic response of the whole head/neck system (d).

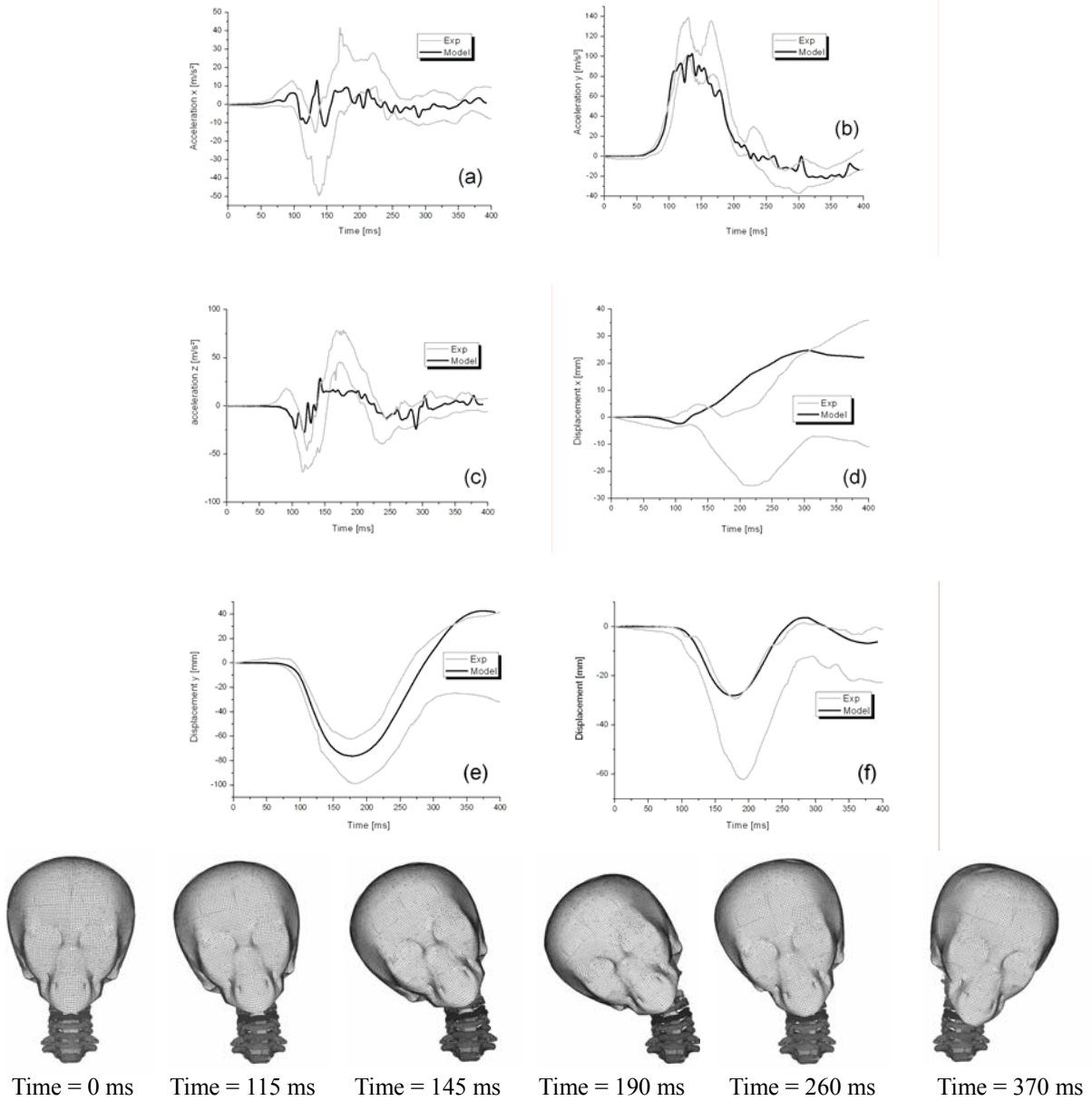
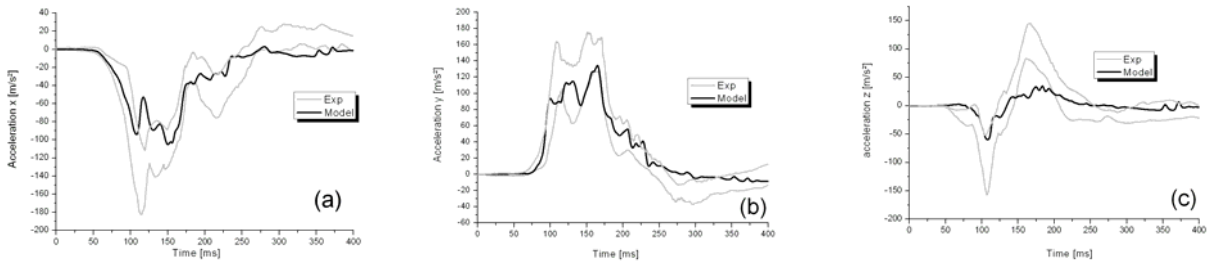


Figure 11: Results under lateral impact: X-axis (a), Y-axis (b), Z-axis (c) linear head acceleration, X-axis (d), Y-axis (e), Z-axis (f) head displacement and kinematic response of the whole head/neck system (g).



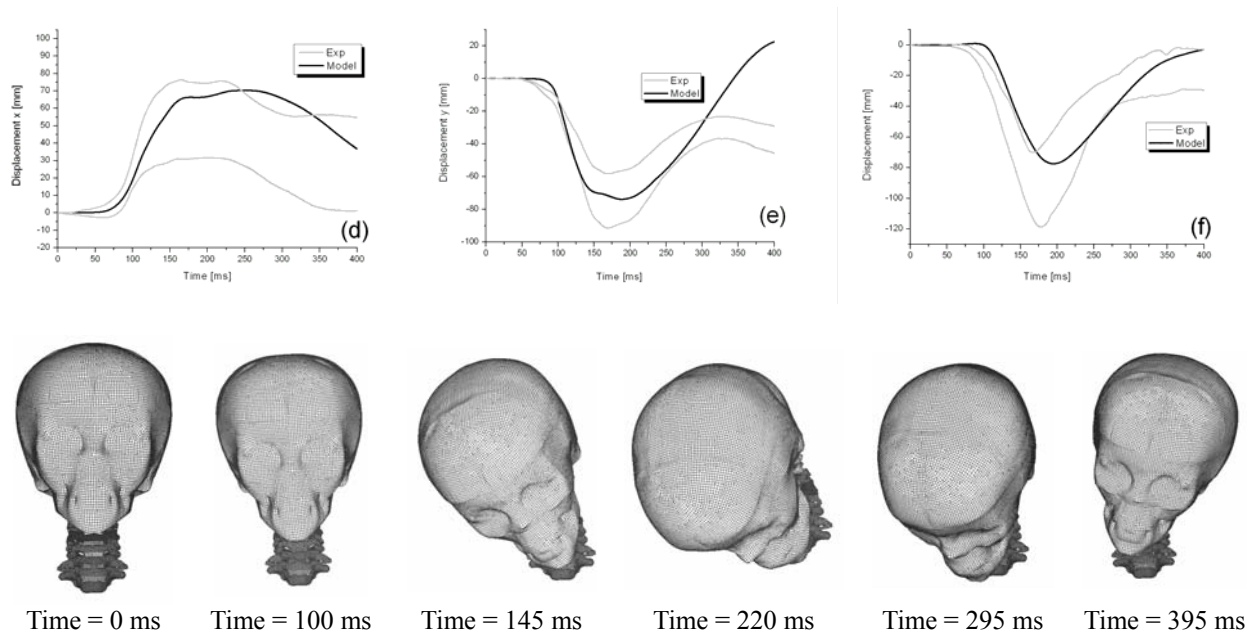


Figure 12: Results under oblique impact: X-axis (a), Y-axis (b), Z-axis (c) linear head acceleration, X-axis (d), Y-axis (e), Z-axis (f) head displacement and kinematic response of whole head/neck system (g).

For the rear impact, only 23% of the global acceleration curve is inside the corridor. Errors in terms of x-axis and z-axis displacement reach up to 52% and 46 % respectively, showing a less accurate response.

For the lateral impact, there is globally a good correlation between the FEM and the corridors up to 88% in terms of x-axis acceleration being in the corridor. Only the z-axis displacement is slightly underestimated with 25% of the curve inside the corridor.

Finally, for the oblique impact, the FEM correctly reproduces acceleration of the centre of gravity of the head with only 30% errors in terms of y-axis acceleration. For x-axis and z-axis acceleration, respectively 55% and 57 % of the curves are inside the corridors. 62% of the points calculated concerning displacement along axis z are inside the corridor. For x axis and y axis displacement, errors reach up to 50 and 58% respectively.

3 Discussion

For ethical reasons human child FE model validation is and will be a difficult or even impossible task in the future. However helps to the scaling methods, FE modelling remains a powerful tool for injury mechanism investigation. If this limitation linked to the model validation procedure is effective, it should be recalled here that children anthropometric test dummies are validated under similar conditions and are routinely used in child restraint system evaluation. It is supposed that in a near future, more detailed numerical models such as the one developed in the present study will enable a more detailed insight to child neck response.

The main originality of the proposed model is to consider a realistic and detailed geometry reproducing the child anatomy particularity. By adding effort at geometrical level, to knowledge from adult neck biomechanics and mechanical properties scaling the authors are convinced that children models can be provided and extensively used under accidental circumstances in order to extract more realistic injury criteria than dummies can.

Beside this optimistic point of view, a number of limitation linked to the present study should be addressed. In addition to the validation issue, important lack of data related to neck tissue and constitutive laws must be mentioned.

The objective of this model is to predict the kinematics of the different parts of the head neck structure, and to obtain forces and elongations of each ligament as well as relative vertebrae motions at this parameters are supposed to be directly related to non severe neck injury. Vertebrae fracture is therefore out of consideration. Improvement in this area will probably be possible in the future.

Concerning the quality of the validation, it should be pointed out that the model response here and there runs out of the corridor. This typically appears in model validation under dynamic loading demonstrating that realistic model is provided even if not 100% validated.

4 Conclusion

Based on medical images of a three year old child neck a detailed neck FE model is proposed including realistic vertebra geometry, intervertebral discs and ligaments. Constitutive laws considered for the different tissue were obtained by scaling down adult mechanical data from the literature. Validation of the model was performed under frontal, lateral, oblique, and rear impact tests reported in the literature for adults and scaled down as well. The proposed model is ready for real world accident reconstruction involving children in order to investigate neck injury criteria for the three year old child neck

References

- [1] Ewing, C., Thomas, D., Patrick, L., Beeler, G. and Smith, M. (1968) Dynamic response of the head and neck of the living human to -Gx impact acceleration. Proc. 12th Stapp Car Crash Conference, pp. 424-439. Society of Automotive Engineers, Warrendale,

PA. Paper 680792

- [2] Ewing, C., Thomas, D., Lustick, L., Muzzy, III W., Willems, G. and Majewski, P. (1977) Dynamic response of the human head and neck to +Gy impact acceleration. Proc. 21st Stapp Car Crash Conference, pp. 549-586. Society of Automotive Engineers, Warrendale, PA. Paper 770928
- [3] Prasad, P., Kim, A. and Weerappuli, D.P.V. (1997) Biofidelity of Anthropomorphic Test Devices for Rear Impact. Proc. 41st Stapp Car Crash Conference, pp. 387-415. Society of Automotive Engineers, Warrendale, PA. Paper 973342
- [4] Kumaresan S, Yoganandan N, Pintar FA (1997) Age specific pediatric cervical spine biomechanical responses: three dimensional nonlinear finite element models. In: Proceedings of 26th STAPP car crash conference, pp 31-61
- [5] Mizuno K, Deguchi T, Furukawa K, Miki K (2004) Development of three-year-old child human FE model. In: IRCOBI conference, Graz, pp 335-336
- [6] Dupuis R, Meyer F, Deck C, Willinger R, Three-year-old child neck finite element modelization, Eur J Orthop Surg Traumatol (2006) 16: 193-202
- [7] Irwin, A. and Mertz, H. J. (1997). Biomechanical basis for the CRABI and hybrid III child dummies, SAE paper 973317
- [8] Chazal J, Tanguy A, Bourges M, Gaurel G, Escande G, Guillot M, Vanneuville G (1985) Biomechanical properties of spinal ligaments and a histological study of the supraspinal ligament in traction. J Biomech 18(3):167-176
- [9] Yoganandan, N., Kumarasan, S. and Pintar, S.A. (2001) Biomechanics of the cervical spine part 2. cervical spine soft tissues responses and biomechanical modelling. Clinical Biomechanics 16(1) : 1-27
- [10] Yoganandan N, Pintar FA, Kumaresan S, Gennarelli TA (2000) Pediatric and small female neck injury scale factor and tolerance based on human spine biomechanical characteristic. IRCOBI conference, Montpellier, 21-23 Sep 2000
- [11] Deng Y-C, Goldsmith W (1987) Response of a human head/ neck/upper-torso replica to dynamic loading-II. Analytical/numerical model. J Biomech 20(5):487-497
- [12] Astori, P. and Raballo, M. (1998) Multy-Body Numerical model of the Human Neck. Proc. Of the Int.Crashworthiness Conference pp 63-72
- [13] Dauvilliers, F. (1994) Modélisation Tridimensionnelle et Dynamique du Rachis Cervical. PhD Thesis, ENSAM Paris
- [14] Happee, R., Hoofman, M., Van den Kroonenberger, A.J., Morsink, P. and Wisman J. (1998) A Mathematical Human Body Model for Frontal and Rearward Seated Automotive Impact Loading. Proc. 42nd Stapp Car Crash Conference, pp. 75-88. Society of Automotive Engineers, Warrendale, PA. Paper 983150
- [15] Meyer F., Bourdet N., Deck C., Willinger R. (2004) Human Neck Finite Element Model Development and Validation against Original Experimental Data. Stapp Car Crash Journal, Vol., pp. 177-206

Tables

Table 1: Meshing criteria allowing the calculation time to be optimised.

<i>Criterion</i>	<i>Values</i>
<i>Length min.</i>	2.25 mm
<i>Length max.</i>	3 mm
<i>aspect ratio</i>	[1-2]
<i>warpage</i>	[0-5]
<i>angle quad (*)</i>	[70-110]
<i>angle tria (*)</i>	[50-80]
<i>Jacobien</i>	[0.7-1]
<i>% of trias</i>	6

Table 2: Coefficients used to define the adult ligaments constitutive laws (Chazal 1985). The rupture strengths are taken from Yoganandan (2001).

Ligaments	α_1		α_2		α_3			
	$\epsilon_1/\epsilon_{3max}$	F_1/F_{3max}	$\epsilon_2/\epsilon_{max}$	F_2/F_{3max}	ϵ_{3max} C2-C5	F_{3max} C2-C5	ϵ_{3max} C5-T1	F_{3max} C5-T1
ALL	0.21	0.11	0.78	0.87	0.308	92.8	0.354	145.2
PLL	0.25	0.12	0.77	0.89	0.182	71.1	0.341	188.2
FL	0.28	0.21	0.76	0.88	0.77	121.5	0.884	129.1
ISL	0.3	0.17	0.75	0.87	0.609	38.6	0.681	38.6
CL	0.26	0.15	0.76	0.88	1.41	119.7	1.16	181.1
<i>Upper cervical spine ligaments</i>	0.26	0.15	0.76	0.88	1	-	1	-

Table 3: Geometrical scaling factors for head and neck of the 3 YOC.

	Scale Factor			
	λ_x	λ_y	λ_z	λ_m
Head	0.876	0.876	0.876	0.672
Neck	0.637	0.637	0.637	0.259

Table 4: Cervical vertebrae inertial properties applied to the center of gravity of each body segment

Name	Mass [g]	Ixx [Kg.cm ²]	Iyy [Kg.cm ²]	Izz [Kg.cm ²]
Head	3200	130	180	120
T1	78	0.846	0.626	0.129
C7	58	0.763	0.328	0.965
C6	58	0.763	0.328	0.965
C5	50	0.636	0.210	0.753
C4	56	0.773	0.221	0.897
C3	70	0.816	0.325	1.01
C2	86	0.902	0.662	1.24
C1	57	1.28	0.36	1.58